Journal of the European Ceramic Society 17 (1997) 1133–1141

PII: S0955-2219(96)00217-8
0955-2219/97/$17.00

Grain Growth in Ultrafine-Grained Y-TZP Ceramics

C. D. Sagel-Ransijn, A. J. A. Winnubst, A. J. Burggraaf and H. Verweij

University of Twente, Faculty of Chemical Technology, Laboratory for Inorganic Materials Science, Enschede, The Netherlands

(Received 23 July 1996; revised version received 20 September 1996; accepted 21 October 1996)

Abstract

Grain growth in dense ultrafine-grained (120–600 nm) tetragonal ZrO_2–Y_2O_3 ceramics is studied as a function of temperature. At all temperatures investigated both segregation and phase partitioning occur. It is argued that at temperatures ≤ 1150°C grain growth is not significantly inhibited by solid solution drag or by phase partitioning. At higher temperatures the grain growth behaviour can be explained by the models of solid solution drag and/or phase partitioning depending on conditions. © *1997 Elsevier Science Limited.*

1 Introduction

In polycrystalline tetragonal zirconia (TZP) ceramics high strength and toughness are combined.[1] These excellent mechanical properties are, *inter alia*, related to a stress-induced martensitic transformation of the metastable tetragonal to the monoclinic phase.[2] In order to retain the tetragonal phase at room temperature the grain size must be kept below a critical value. For zirconia powders doped with 3 mol% Y_2O_3 the ceramic grain size must be less than 0·8 μm to remain fully tetragonal at room temperature.[3] However, this critical grain size is much smaller (about 0·3 μm) when the ceramic has to remain tetragonal after aging in water at elevated temperatures.[4–6]

In order to control grain growth in a ceramic body during processing, a profound knowledge of grain growth parameters is needed. Control of grain growth is achieved by controlling the underlying process, which is, in dense ceramics, grain boundary migration.

Grain growth of dense zirconia ceramics depends on composition and phase content. Three models have been proposed to account for the sluggish grain growth in some TZP ceramics. The model of Lee and Chen[7] is based on the differences in grain boundary energy between tetragonal and cubic grains. According to Theunissen *et al.*[8–10] the sluggish grain growth is attributed to impurity drag. Lange[11] claims that grain growth in TZP ceramics is restricted by phase partitioning. No consistent explanation of the grain growth behaviour in TZP materials has been given up to now.

Grain growth kinetics in dense ceramics at low temperatures, which is interesting for the preparation of nanostructured materials, is not often reported in the literature. To obtain insight into the grain growth kinetics, grain growth experiments were performed on dense ultrafine-grained Y–TZP ceramics between 1070 and 1375°C. The temperature of 1070°C was the lowest where densities ≥96% could be achieved. A further aim of this research is to obtain a better insight into the dominant grain growth-controlling mechanism at different sintering temperatures.

2 Theory of Grain Growth

In general the grain growth rate $\mathrm{d}\bar{D}/\mathrm{d}t$ (with $\bar{D}$ the average grain size) is directly proportional to the instantaneous average rate $\bar{u}_b$ of grain boundary migration in the structure.[12] Thus:

$$\mathrm{d}\bar{D}/\mathrm{d}t \sim \bar{u}_b \tag{1}$$

The term $\bar{u}_b$ can be represented in terms of a force–mobility product:

$$\bar{u}_b = M_b F \tag{2}$$

where F is the net driving force, and all factors arising from migration of matter are assembled in the mobility term M_b. The driving force for boundary migration, F, in ceramics is most commonly derived from the pressure gradient, ΔP, across the boundary arising from its curvature given by:

$$\Delta P = 2\gamma \left(\frac{1}{r_1} + \frac{1}{r_2} \right) \tag{3}$$

where γ is the grain boundary energy and r_1 and r_2 are two main radii of curvature describing the boundary surface.

From the various mechanisms available in the literature concerning grain growth control, three mechanisms will be discussed in detail because they are claimed to have an important role in the case of Y-TZP.

2.1 Effect of intrinsic properties

Differences in grain growth between cubic and tetragonal zirconia can be expected because of differences in intrinsic properties such as grain boundary energy or diffusion coefficients which affect ΔP (eqn (3)) and $\bar{u}_b$ (eqn (2)).

Lee and Chen[7] have shown by measurements of dihedral angles and rate constants in two-phase zirconia that the differences in grain boundary energy cannot account for the large difference in rate constant between cubic and tetragonal zirconia.

Mass transport in fluorite-structured oxides is closely related to their defect structure. In pure ZrO_2, where Schottky defects are the most common defects, the following equilibrium exists:

$$O \rightleftarrows V_{Zr}'''' + 2V_0^{\cdot\cdot} \tag{4}$$

The equilibrium constant K can be represented as:

$$K = [V_{Zr}''''][V_0^{\cdot\cdot}]^2 \tag{5}$$

When zirconia is doped with yttria the defect reaction can be represented as:[13]

$$YO_{1.5} \rightarrow Y_{Zr}' + \frac{1}{2}V_0^{\cdot\cdot} + \frac{3}{2}O_O^x \tag{6}$$

Hence, doping zirconia will increase $[V_0^{\cdot\cdot}]$ and thus, according to eqn (5), decrease $[V_{Zr}'''']$. Because diffusion strongly depends on the number of (metal) vacancies,[8] it could be expected that the chemical diffusion coefficient will be lower in the case of cubic zirconia with a high yttria content resulting in a smaller grain growth rate. However, this is contrary to what is found experimentally.

It can be concluded that the smaller grain growth rate in tetragonal zirconia as compared to cubic zirconia is not solely due to intrinsic properties like grain boundary energy or vacancy concentration.

2.2 The impurity drag mechanism

Another mechanism for grain growth control is based on the concept of solution drag. The drag effect arises from any preferred segregation of an impurity either to or from the grain boundary area, because of size or charge differences.[12,14] The free energy of the system increases when the grain boundary breaks away from this impurity cloud. Thus the grain boundary tends to drag the cloud of impurities along with it, diminishing the driving force, F, and severely retarding grain growth.

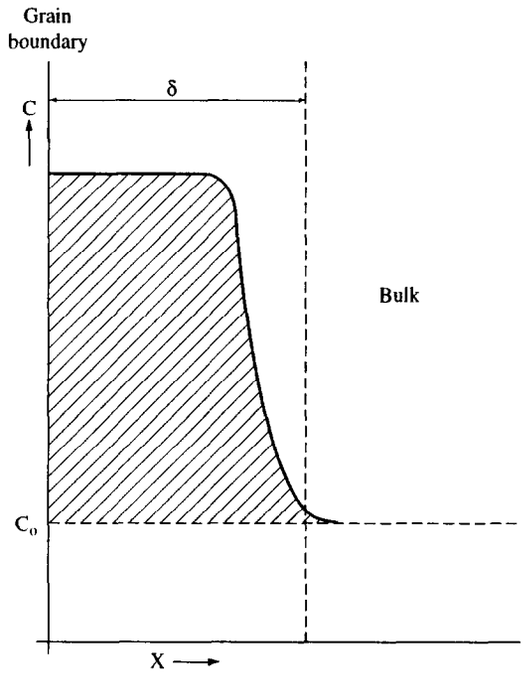

Fig. 1. Schematic representation of the concentration profile of the segregated solute atoms in the grain boundary area. Taken from Ref. 10.

If impurity drag is applicable as a grain-growth controlling mechanism, the net driving force is composed of the driving force for grain growth minus the dragging force (i.e. $F=\Delta P - P_i$). By inserting this in eqns (1) and (2) the following equation is obtained:

$$d\bar{D}/dt = M_b(\Delta P - P_i) \tag{7}$$

According to Theunissen[8] (based on Cahn's work[15]), with segregation as the only dragging force, the dragging force is proportional to the area under the curve of the impurity concentration as a function of the distance to the grain boundary. This situation is shown in Fig. 1. As a first approximation Theunissen uses the situation where the impurity segregation is constant over a certain distance (δ) (measured from the grain boundary) and then decreases rapidly to the bulk level C_0. Theunissen states that if the grain boundary width (δ) in a series of experiments is the same, the dragging force is determined by the segregation factor C_{gb}/C_0 where C_{gb} is the concentration at the grain boundary and C_0 is the bulk impurity concentration.

Hwang and Chen[16] confirmed the impurity segregation and explained the dragging behaviour of different dopants using a space charge concept.

2.3 Phase partitioning

Phase partitioning, as a third mechanism for grain growth control has been proposed by Lange.[11] It is known that the lattice parameters of the tetrag-

onal structure depend on the yttrium content.[17] For this reason, Lange[11] considered each grain as a 'separate phase' with an identical structure, but a slightly different composition, and thus a grain with different lattice parameters. In such a 'polyphase' material, the growing grain must abruptly change its lattice parameters at the location where its grain boundaries move into adjacent grains with different composition. In that case, the moving grain boundary leaves behind a coherent interface at the location where the lattice parameters change. The different lattice parameters on the two sides will produce strain energy and a dragging force is correlated to this. No arguments were given to support this statement.

The effect of the coherent interfaces, which are left behind, on grain shrinkage or growth was estimated by Lange by determining the net driving 'stress'. The restraining 'stress' associated with the coherent interface was related to its strain energy density, $k\epsilon^2E/2$. where k is a dimensionless proportionality constant which is expected to be identical for all boundaries and compositions,[11] ϵ is a scalar associated with the change in the lattice cell volume across the coherent interfaces and E is Young's modulus (assumed to be identical for all grains). There are no arguments (nor derivation) given to relate restraining stress to strain energy. A value for k is not reported in the literature. The net driving force for grain growth determined by phase partitioning is given then by:

$$P = \Delta P - P_p = 2\gamma\left(\frac{1}{r_1} + \frac{1}{r_2}\right) - \frac{k\epsilon^2E}{2} \qquad (8)$$

The equation shows that the formation of the coherent interface reduces the driving 'force' for grain growth. The larger the differential lattice parameters, the larger the restraining 'force'. Lange does not give an estimate of the minimum amount of phase partitioning required in order to restrain grain growth and thus this theory cannot be evaluated in a quantitative way by experiments.

3 Experimental Procedure

3.1 Sample preparation

Nanocrystalline zirconia powder (crystallite size 8 nm) with 5 at% Y on the Zr-site (ZY5) was synthesized by a gel-precipitation technique using metal chlorides as precursor materials. The ethanol-washed gel was hydrothermally crystallized at 200°C and heat treated at 400°C. This method yields very sinter-reactive powders with a low degree of agglomeration. Details of this synthesis method can be found elsewhere.[18]

The powder was isostatically pressed at 400 MPa and sintered at temperatures ranging from 1070 to 1375°C (heating rate 2°C min^{-1}; cooling rate 4°C min^{-1}). Samples were sintered non-isothermally or with an isothermal dwell up to 400 h. Each sample underwent only one heating and cooling cycle. In order to have a good estimate of the grain size at the onset of the isothermal part of the sintering process, three green compacts were heated to the desired temperature (1150, 1250 and 1375°C) and then directly cooled down without isothermal hold. The grain sizes of those samples were used as D_0 values for the isothermal runs at the same temperature. At 1070°C the minimum time required to obtain a dense (96%) ceramic is 10 h and this sample was used to estimate D_0. In all cases, dense samples with a relative density of 96% or more and a grain size larger than 100 nm were obtained. The residual porosity was mainly in the form of flaws in the ceramic. Examination of the microstructures showed no evidence for pinning of the grain boundary by residual pores.

3.2 Analysis

Grain sizes (D) in sintered specimens were analysed by the lineal intercept technique from SEM (Hitachi S800) micrographs of polished, thermally etched cuts using $D = 1{\cdot}56\ L$,[19] where L is the average lineal intercept. No attempt was made to treat the tetragonal grains separately from the cubic grains. The surfaces of the SEM specimens were coated with Au or Au/Pd to prevent charging. It has been checked with HRTEM (Philips CM30 TWIN/(S)TEM) that no grains smaller than those observed with SEM are present in the sintered compact.

The relative amount of cubic structure of the dense ceramics was analysed by XRD (Philips PW 1710) in the range 70–76° (2Θ). Corrections of integral line intensities were only made for $K_{\alpha1}/K_{\alpha2}$ splitting. The $K_{\alpha1}$ peak was used for phase analysis. A selected area electron diffraction option (SAED) mounted on the HRTEM fitted with a double goniometer stage (± 45°) at 300 keV and an aperture of 0·1–0·2 μm has been used to analyse the phase content of single grains. The temperature of the specimen was well below 100°C during analysis and heating by the electron beam was considered to be negligible. The spatial resolution of the HRTEM was 2·3 Å.

The specimens for HRTEM/SAED were prepared by careful polishing, dimple grinding and ion thinning with Ar^+ ions with an energy of 5 keV.

Table 1. Sintering conditions and grain sizes (heating rate 2°C min^{-1}; cooling rate 4°C min^{-1})(Porosites ≤ 4%)

Sinter temperature (°C)	*Sinter time (h)*	*Grain size (nm)*
1070	10	127 ± 4
	50	128 ± 4
	230	154 ± 9
	400	151 ± 2
1150	0	131 ± 5
	1	157 ± 3
	10	147 ± 5
	50	187 ± 2
	100	200 ± 11
1250	0	193 ± 8
	1	227 ± 3
	10	234 ± 3
	40	267 ± 10
	60	271 ± 6
	100	279 ± 4
1375	0	298 ± 17
	1	312 ± 15
	10	362 ± 17
	20	426 ± 10
	50	501 ± 4
	70	528 ± 29
	85	525 ± 32
	100	614 ± 26

4 Results

4.1 Grain size analysis

Table 1 reports the sintering conditions of all specimens and their grain sizes. In all cases the grain size is rather uniform as is shown in Fig. 2 which shows the material sintered for 100 h at 1375°C.

Isothermal grain growth behaviour can be described with the kinetic growth equations of the general form:[12]

$$D^n - D_o^n = K(t - t_o) \quad (9)$$

In the above equation, n is a constant for a given grain growth mechanism, D is the grain size at time t, D_0 is the reference grain size at time t_0 (see section 3·1), and K is a temperature-dependent constant.

Grain growth at 1070°C is extremely slow. After 10 h sintering at this temperature the grain size was between 120 and 130 nm and this was taken as the value for D_0. After 400 h sintering at 1070°C the grains had only grown to a size of 150 nm. The relatively low accuracy (5%) of the grain size measurements together with the extremely sluggish grain growth makes it impossible to use the few data obtained at 1070°C for accurate grain growth analysis.

The grain size data of 1150, 1250 and 1375°C were plotted in a log to log graph. The regression coefficients for the different temperatures and n values are shown in Table 2. The differences in regression coefficients for the various n values (1–4) were not significant enough to decide on a certain grain growth mechanism. However, values of $n = 1$ (anomalous grain growth) and $n = 4$ (pore drag-controlled grain growth) are very unlikely and are disregarded, because of the experimentally observed rather narrow grain size distribution and the small fraction of porosity (2–4%) (Fig. 2, no pores at grain boundaries), respectively. A value of $n = 2$ suggests normal grain growth. A value of $n = 3$ suggests a solid solution drag-controlled grain growth.

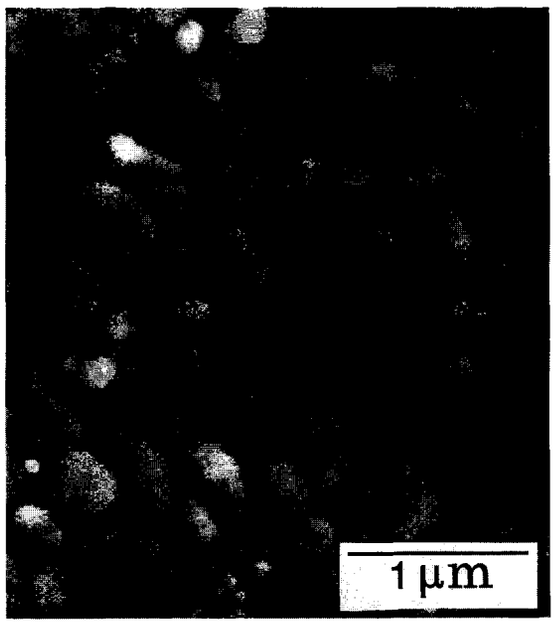

Fig. 2. SEM picture of sample sintered 100 h/1375°C showing a narrow grain size distribution.

In Fig. 3 it is shown that at all temperatures investigated, the grain growth kinetics can be fitted with $n = 2$ or $n = 3$.

4.2 Phase analysis

For phase determinations by XRD the cubic peak ($(400)_c$) and the tetragonal peaks ($(400)_t$ and $(004)_t$) were used. It should be noted that small fractions of either cubic phase in a predominantly tetragonal material or vice versa could not be detected because of mutual overlap of discriminating diffraction peaks. As illustrated in Fig. 4, only the $(400)_t$ and $(004)_t$ diffraction peaks are observed for

Table 2. Regression coefficients for ZY5 sintered at different temperatures calculated for different n values

Temperature	*Regression coefficient*			
	n=1	n = 2	n = 3	n = 4
1150°C	0·9793	0·9808	0·9820	0·9829
1250°C	0·9575	0·9562	0·9550	0·9539
1375°C	0·9942	0·9946	0·9936	0·9917

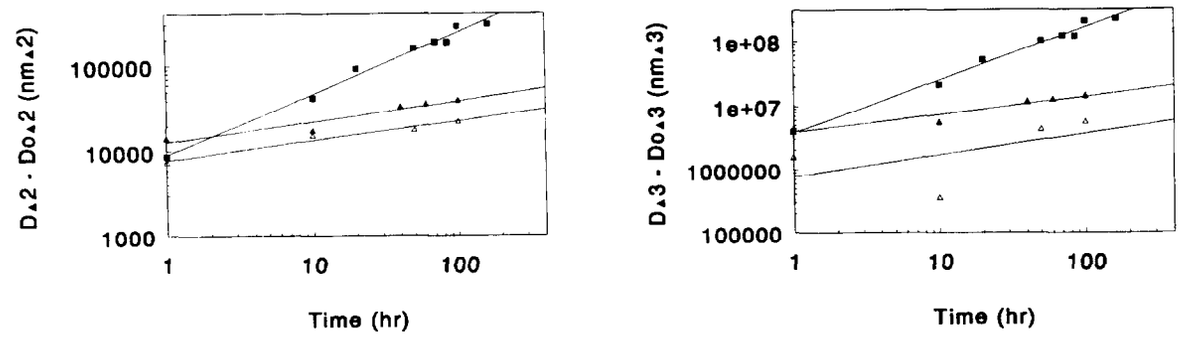

Fig. 3. Grain growth kinetics at (Δ) 1150, (▲) 1250 and (■) 1375°C. A: $n = 2$; B : $n = 3$.

samples heated for times up to 100 h at low temperatures (1070 and 1150°C) or short times (0 h) at 1250 and 1375°C. The onset of the development of a $(400)_c$ peak can be observed for the sample heated for 100 h at 1250°C. After heating for 100 h at 1375°C the cubic structure was identified by the presence of a clear $(400)_c$ diffraction peak. The amount of cubic phase in this material is estimated to be approximately 10% using the equation of Paterson and Stevens.[20] The XRD results indicate that the cubic phase could only be found at a sintering temperature of 1250°C or higher. Thus, phase partitioning takes place at those temperatures.

In addition, SAED was performed in order to observe whether minor amounts of cubic material exist in the sintered specimens. These results can only be used qualitatively because only a few grains were analysed accurately for each sample. In all cases, with SAED, grains with two different crystallographic symmetries could be detected. Figure 5A shows a typical tetragonal spot pattern, whereas Fig. 5B shows a spot pattern typical for a hexagonal symmetry. The spot patterns were interpreted by the zone axis method.[21] Most tetragonal SAED patterns could be assigned to a tetragonal structure ('tetragonal 1'), whereas most hexagonal SAED patterns could be assigned to a cubic structure. In a number of cases the hexagonal patterns could not be indexed as a cubic but as a tetragonal symmetry. This tetragonal phase is different from the first directly observed one.

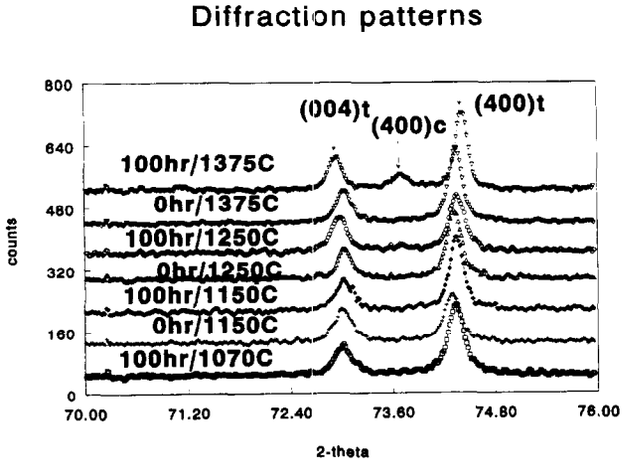

Fig. 4. XRD results. The cubic structure is visible for the cases 100 h/1250°C and 100 h/1375°C at $2\Theta = 73{\cdot}6°$.

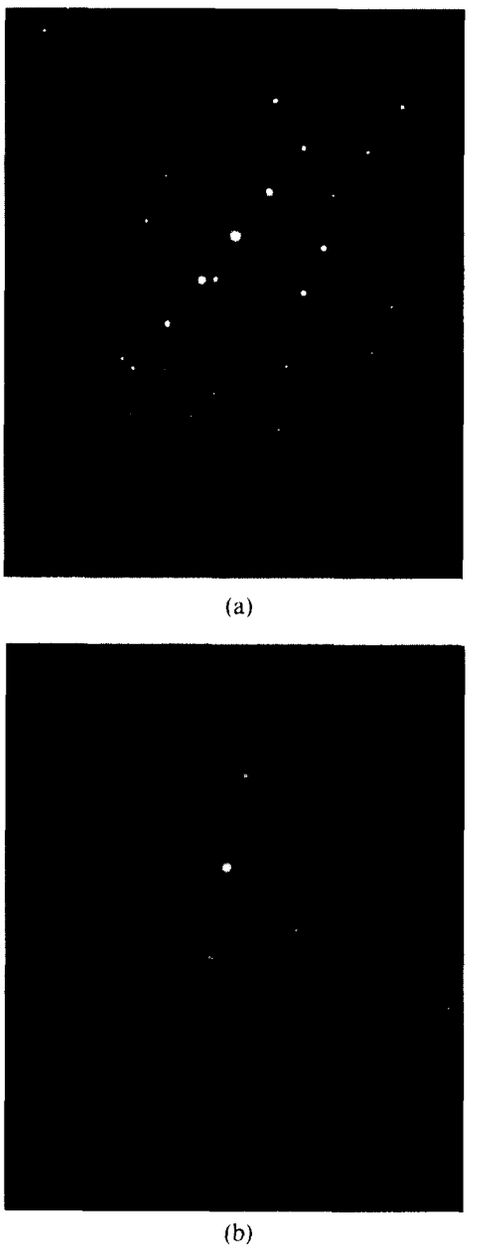

Fig. 5. Diffraction pattern showing (a) tetragonal and (b) hexagonal structure.

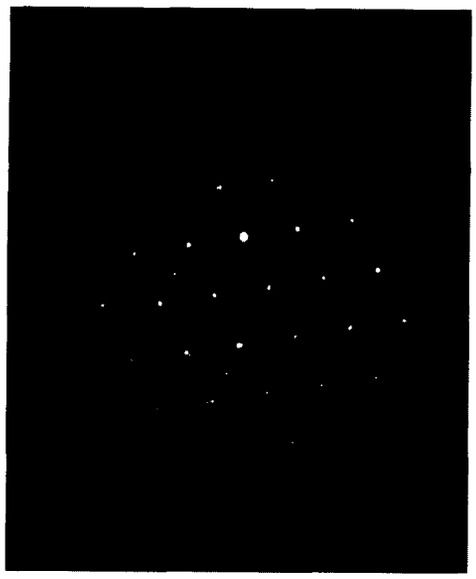

Fig. 6. Diffraction pattern showing 'tetragonal 2' structure.

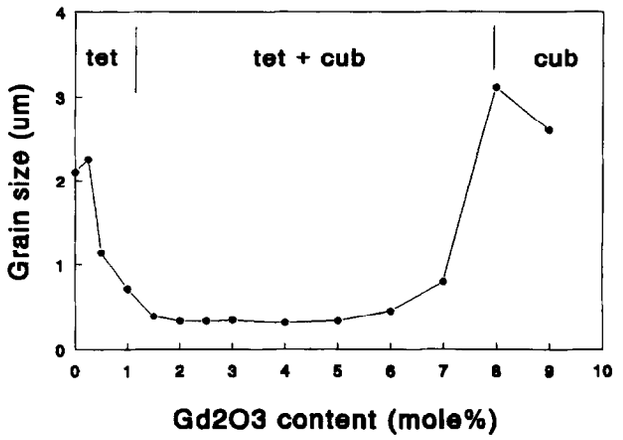

Fig. 7. Grain size of Gd_2O_3–ZrO_2 material sintered at 1400°C for 1 h. Taken from Ref. 12.

We will call this phase 'tetragonal 2'. As an example in Fig. 6 the spot pattern of a 'tetragonal 2' structure in ZY5 sintered 400 h/1070°C is shown. The occurrence of a cubic phase was also confirmed by calculating the angle between pairs of planes.[21]

The hexagonal spot pattern of the 'tetragonal 2' structure suggests that the tetragonality (c/a ratio) of those grains is small. In general the tetragonality decreases with increasing dopant content until a cubic structure is obtained.[22] Thus, the occurrence of both 'tetragonal 2' and other structures on the SAED photographs implies that the yttrium is inhomogeneously distributed from grain to grain. From the SAED results it can be concluded that some phase partitioning is already developing at a temperature as low as 1070°C.

5 Discussion: Grain Growth Kinetics at Increasing Temperatures

5.1 Grain growth at 1070°C

Studies on grain growth kinetics of dense Y-TZP are scarce. Theunissen *et al.*[8,10] reported on the grain growth kinetics of dense Y-TZP at 1000°C. They found that the grain growth data could best be fitted with $n = 3$, suggesting a solid solution drag-controlled grain growth. A necessary condition for solid solution drag is segregation of one of the components of the solid solution. The interface composition of ZY4, ZY13 and ZY17 sintered at temperatures around 950°C as analysed by AES amounts to ZY32–ZY34 (ZY_x means x at% Y on the 2R-site).[14] This corresponds to a Y/Zr ratio of 0·3. Boutz *et al.*[23] found for ZY5 at 10 h/1150°C a similar Y/Zr ratio at the grain boundary. From those results it can be concluded that the Y/Zr ratio at the grain boundary between 950 and 1150°C amounts to 0·3.

SAED measurements revealed that some cubic grains are present in the ceramic material sintered at 1070°C. Thus, at 1070°C both yttrium segregation and a small amount of phase partitioning take place.

At 1070°C normal grain growth kinetics ($n = 2$) most likely take place. As a result of the small grain size the driving force (ΔP) for grain growth is large. The small grain size means that the contribution of a 'dragging' force or a 'phase partitioning' force is relatively small, if present. The sluggish grain growth at 1070°C must therefore be ascribed to the low sintering temperature and the narrow grain size distribution.

5.2 Grain growth at 1150°C

At 1150°C no cubic phase was detected by XRD. SAED, on the other hand, showed in all compacts some cubic phase. Furthermore, grains with different tetragonality were found by SAED and thus a 'polyphase' material is present at 1150°C. It is, however, not likely that the strain energy arising from phase partitioning limits the grain growth at this temperature as will be discussed below.

Grain growth at 1150°C has been investigated by Boutz *et al.*[24] They compared the grain size of ZY5, ZY4Cex (x = 2, 4, 6, 8) and ZCe12 at a temperature of 1150°C. For their experiments they used the same type of nanocrystalline powders (crystallite size 8–10 nm) with a low degree of agglomeration. After 10 h/1150°C the above-mentioned compositions have an identical grain size (0.2 μm) and a high density (>95%). ZY5 is known to lie in the tetragonal and cubic phase field.[25] In the present work it is shown that phase partitioning is occurring at 1150°C for ZY5. On the other hand, ZCe12 lies in the single tetragonal phase field.[22] This means that no phase partitioning can occur in ZCe12. Because both ZY5 and ZCe12 have the same grain size after sintering for 10 h/1150°C and assuming comparable D_0 values (powder proper-

ties are similar), it is concluded that grain growth at 1150°C is not limited by strain energy arising from phase partitioning.

To investigate whether grain growth is controlled by solid solution drag Boutz *et al.*[24] measured the segregation of yttrium and cerium to the grain boundaries for ZY5 and ZY4Ce*x* by XPS. In all cases it was found that the grain boundaries were enriched in yttrium by a factor of ≈2 with respect to the bulk composition. (The difference in segregation factors found with AES and XPS is caused by the different information depths of the two methods.[24]) In Y,Ce-TZP no or a very small amount of segregation of cerium was observed as is in accordance with the results of Hwang *et al.*[16] Thus grain sizes in ZY5, ZY4Ce*x* and ZCe12 are the same despite the fact that yttrium does and cerium does not segregate to the grain boundary at 1150°C. Assuming comparable D_0 values (powder properties are similar), this means that grain growth at 1150°C is probably not limited by segregation effects.

In conclusion, at temperatures between 1000 and 1150°C grain growth inhibition by segregation or by phase partitioning does not play an important role. Grain growth in this temperature regime is most probably only determined by the magnitude of the driving force and n should be 2.

5.3 Grain growth at 1250 and 1375°C

After sintering at 1250 or 1375°C, phase partitioning has occurred as was confirmed by XRD and SAED.

Leung *et al.*[26] studied the phase relations, partitioning reactions, and grain growth of ZrO_2 Gd_2O_3 with energy dispersive spectroscopy (EDS) as a major technique. The grain size as a function of composition for the ZrO_2–Gd_2O_3 material is given in Fig. 7. The shape of the curve is similar to that of ZrO_2–Y_2O_3 as measured by Lange.[27] Leung *et al.*[26] measured the Gd_2O_3 content of different grains for ZrO_2–3 mol% Gd_2O_3 material heated to 1400°C and held for different periods. The amount of Gd_2O_3 in the tetragonal grains decreased with increasing time and became constant after 200 h at 1400°C. Cubic grains (8 mol% Gd_2O_3) were rarely found in specimens heat-treated for short periods (<5 h). The volume of cubic grains increased with time. Based upon the EDS results Leung *et al.*[26] concluded that phase partitioning in their material was complete after 200 h/1400°C, which resulted in a two-phase material. The theory of grain growth inhibition by phase partitioning predicts that when phase partitioning is complete, tetragonal grain growth rate should be increased. Leung *et al.*[26] found, however, that slow tetragonal grain growth continues even after phase partitioning is completed which is confirmed by Allemann *et al.*[28] who found similar results for other zirconia ceramics. Preliminary evidence obtained by Leung *et al.*[26] suggested that similar compositions in the ZrO_2–Y_2O_3 system exhibited partitioning kinetics similar to ZrO_2–Gd_2O_3. These results might indicate that phase partitioning is not the cause of the *continuing* slow grain growth.

The grain growth in the system described in this work is rather constant with time (see Fig. 3). The equilibrium amount of cubic phase in ZY5 is according to the phase diagram of Scott[25] approximately 16%. The material sintered for 100 h at 1375°C contains 10% cubic phase. Thus, phase partitioning is not completed in the presently investigated materials and grain growth inhibition by phase partitioning cannot be excluded by *this* argument. In conclusion, the strain energy model arising from phase partitioning can qualitatively account for the smaller grain growth rate in the two-phase tetragonal + cubic field in comparison to that in the single-phase domain (either tetragonal or cubic). However, if grain growth is only suppressed by phase partitioning, a reason for the differences in grain growth in the single tetragonal phase-field cannot be given nor can the slow tetragonal grain growth after complete phase partitioning be explained.

Now it will be discussed whether the drag mechanism caused by segregation of main component(s) can account for the limited grain growth found at 1250 and 1375°C. In Ref. 26 the relevance of the solute-drag model is questioned when an amorphous phase resides between the grains. It is known that the second phase film reduces the mobility of the boundary in a similar way as the solid solution situation.[12] In the following it will be argued that although the grain boundary is probably wetted by a small amount of an amorphous 'phase' at the sintering temperature, the rate of grain growth can still be dependent on the solute (segregational) drag. Boutz *et al.*[23,24,29] have shown by TEM the existence of a 0·5–1 nm thick amorphous-like ultra-thin layer. It was found that this layer is strongly enriched in silicon and yttrium. The yttrium enrichment observed at grain boundaries containing this layer is, however, not confined to the amorphous ultra-thin layer alone.[23,24,29] This means that although the dragging effect may be reduced by the presence of some amorphous 'phase', it is still present[12] due to segregation within the bulk.

The effect of yttria addition on grain growth in yttria-doped ceria ceramics was investigated by Upadhyaya *et al.*[30] They found that the grain size in ceria ceramics is inversely dependent on yttria

concentration (1–8 mol% Y_2O_3). All compositions lie in the single phase-field where a solid solution of Y_2O_3 in CeO_2 exists[31] and phase partitioning cannot play a role. Evidently the role of Y_2O_3 is to suppress the grain boundary mobility and retard the kinetics of mass transport during sintering. In Ref. 30 it is argued that in those materials Y segregates to the grain boundary. The size mismatch between Y and Ce is smaller than between Y and Zr and, therefore, the segregation factor Y/Ce should be smaller than that of Y/Zr.[14] The smaller segregation factor is expected to lead to less solid solution drag for the Y_2O_3–CeO_2 system as compared to the Y_2O_Z–ZrO_2 system. Because only grain *size* measurements were performed instead of grain *growth* measurements as in this study, the explanation of grain growth control in yttria–ceria ceramics by solid solution drag is not completely straightforward.

In conclusion it can be stated that the data on grain growth cannot consistently be explained by the strain energy model arising from phase partitioning *or* by the impurity drag mechanism only. Phase partitioning cannot account for the differences in grain size found in the single tetragonal phase field (or in general in a single-phase field like in doped ceria) nor for the slow tetragonal grain growth when phase partitioning is completed. Impurity drag, on the other hand, cannot explain why the grain size abruptly increases when the concentration of yttria is raised above the amount found in the two-phase field. If both mechanisms are cooperative in inhibiting grain growth, then all of the present results can be put into a scheme as shown in the following section to obtain optimum grain growth inhibition.

5.4 Proposed scheme for grain growth

Based on the results it is hypothesized that at all temperatures the driving force for grain growth in zirconia can be described by the following equation:

$$P = \Delta P - P_i - P_p \tag{10}$$

with P the total force, ΔP the force gradient arising from grain boundary curvature, P_i the restraining force through impurity drag and P_p the restraining force through strain energy arising from phase partitioning.

At low temperatures (≤1150°C) grain growth is not inhibited significantly because the grains are very small, resulting in a large ΔP. At higher temperatures both segregation and phase partitioning have been found. At those temperatures a dragging force and a phase partitioning force are cooperative depending on the precise properties of the segregation layer and the distribution of yttrium over the grains.

At increasing temperatures P_i increases with respect to ΔP because of the larger grain sizes involved. A dragging force is, however, lacking when the amount of solvent ions (substitutes in the solid solution) is too low to provide a saturated concentration profile across the complete internal grain boundary surface. Thus maximum dragging by segregation requires an amount of doping ions sufficient to develop the saturation concentration in the layer (Fig. 1). The increasing grain size with decreasing Gd_2O_3 content in the single tetragonal phase-field (Fig. 7) can be explained by the lack of a sufficient amount of solvent ions for segregation.

The force caused by strain energy arising from phase partitioning depends on the distribution of yttrium over the grains. A high inhomogeneity results in a 'polyphase' material and in a strong inhibition of grain growth. The weak point in this theory is that the minimum amount of 'phase partitioning' to obtain effective drag is not given. After a certain heating schedule the 'polyphase' material is converted into an equilibrium two-phase material. In this two-phase material it is not expected that grain growth will be inhibited by strain energy arising from phase partitioning. Thus, the force caused by phase partitioning goes through a maximum. In this two-phase material the growth of the small tetragonal grains is not hindered by the large cubic grains. The growth of the cubic grains is, however, limited by the presence of small tetragonal grains. The grain growth of both phases in the two-phase material can, however, be limited by the dragging force at high temperatures (>1150°C).

6 Conclusions

- At temperatures equal to and below 1150°C grain growth in ultrafine-grained Y-TZP ceramics is not significantly inhibited by (solid solution) segregation or by phase partitioning.
- At temperatures above 1150°C grain growth in Y-TZP ceramics is inhibited by both strain energy arising from phase partitioning and solid solution drag by segregation depending on conditions.
- When phase partitioning is completed, tetragonal grain growth in the two-phase material can only be restricted by drag caused by solid solution segregation. Cubic grain growth is in this case restricted by segregation as well as by the presence of the smaller tetragonal grains.

References

1. Swain, M. V. and Rose, L. R. F., Strength limitations of transformation-toughened zirconia alloys. *J. Am. Ceram. Soc.*, 1986, **69**(7), 511–518.
2. Green, D. J., Hannink, R. H. J. and Swain, M. V., *Transformation Toughening of Ceramics*. CRC Press, Boca Raton, Florida, 1989.
3. Lange, F. F., Transformation toughening; Part 3: Experimental observations in the ZrO_2–Y_2O_3 system. *J. Mater. Sci.*, 1982, **17**, 240–246.
4. Watanabe, M., Jio, S. and Fukuura, J., Ageing behavior of Y_2O_3–PSZ. In *Advances in Ceramics, Vol. 12, Science and Technology of Zirconia II*, ed. N. Claussen, M. Rühle and A. H. Heuer. The American Ceramic Society, Inc., Columbus, Ohio, 1984, pp. 391–398.
5. Chen, S-Y. and Lu, H-Y., Low-temperature ageing map for 3 mol% Y_2O_3–ZrO_2. *J. Mater. Sci.*, 1989, **24**, 453–456.
6. Winnubst, A. J. A. and Burggraaf, A. J., The aging behaviour of ultrafine-grained Y-TZP in hot water. In *Advances in Ceramics, Vol. 24A, Science and Technology of Zirconia III*, ed. S. Somiya, N. Yamamoto and H. Hanagida. American Ceramic Society, Westerville, OH, 1988, pp. 39–47.
7. Lee, I. G. and Chen, I.-W., Sintering and grain growth in tetragonal and cubic zirconia. In *Sintering '87*, ed. S. Somiya *et al.* Elsevier Applied Science, London, 1988, pp. 340–345.
8. Theunissen, G. S. A. M., Microstructure, fracture toughness and strength of (ultra) fine-grained tetragonal zirconia ceramics. PhD thesis, University of Twente, Enschede, The Netherlands, 1991.
9. Winnubst, A. J. A., Theunissen, G. S. A. M., Boutz, M. M. R. and Burggraaf, A. J., Microstructure development during sintering of nanocrystalline tetragonal zirconia. In *Structural Ceramics — Processing, Microstructure and Properties*, ed. J. J. Bentzen, J. B. Bilde-Sørensen, N. Christiansen, A. Horsewell and B. Ralph. Risø National Laboratory, Roskilde, Denmark, 1990, pp. 523–528.
10. Theunissen, G. S. A. M., Winnubst, A. J. A. and Burggraaf, A. J., Sintering kinetics and microstructure development of nanoscale Y-TZP ceramics. *J. Eur. Cer. Soc.*, 1993, **11**, 315–324.
11. Lange, F. F., Controlling grain growth. In *Ceramic Microstructures '86: Role of Interfaces, Materials Science Research Volume 21*, ed. J. A. Pask and A. G. Evans. Plenum Press, New York, 1987, pp. 497–508.
12. Brook, R. J., Controlled grain growth. In *Treatise of Materials Science and Technology, Vol. 9*, ed. F. F. Y. Wang. Academic Press, New York, 1976, pp. 331–364.
13. Weller, M. and Schubert, H., Internal friction, dielectric loss, and ionic conductivity of tetragonal ZrO_2–3% Y_2O_3 (Y-TZP). *J. Am. Ceram. Soc.*, 1986, **69**(7), 573–577.
14. Burggraaf, A. J. and Winnubst, A. J. A., Segregation in oxide surfaces, solid electrolytes and mixed conductors. In *Surface and Near Surface Chemistry of Oxide Material*, ed. J. Nowotny and L.-C. Dufour. Elsevier Science Publishers BV, Amsterdam, 1988, pp. 449–477.
15. Cahn, J. W., The impurity-drag effect in grain boundary motion. *Acta Metall.*, 1962, **10**, 789–798.
16. Hwang, S.-L. and Chen, I.-W., Grain size control of tetragonal zirconia polycrystals using the space charge concept. *J. Am. Ceram. Soc.*, 1990, **73**(11), 3269–3277.
17. Ingel, R. P. and Lewis III, D., Lattice parameters and density for Y_2O_3-stabilized ZrO_2. *J. Am. Ceram. Soc.*, 1986, **69**(4), 325–332.
18. Sagel-Ransijn, C. D., Winnubst, A. J. A., Burggraaf, A. J. and Verweij, H., The influence of crystallization and washing medium on the characteristics of nanocrystalline Y-TZP. *J. Eur. Ceram. Soc.*, 1996, **16**, 759–766.
19. Mendelson, M. I., Average grain size in polycrystalline ceramics. *J. Am. Ceram. Soc.*, 1969, **52**, 443–446.
20. Paterson, A. and Stevens, R., Phase analysis of sintered yttria-zirconia ceramics by X-ray diffraction. *J. Mater. Res.*, 1988, **1**(2), 295–299.
21. Jackson, A. G., *Handbook of Crystallography, for Electron Microscopists and Others*. Springer-Verlag, New York, 1991.
22. Yoshimura, M., Phase stability of zirconia. *Am. Ceram. Soc. Bull.*, 1988, **67**(12), 1950–1955.
23. Boutz, M. M. R., Chen, C. S., Winnubst, L. and Burggraaf, A. J., Characterization of grain boundaries in superplastically deformed Y-TZP ceramics. *J. Am. Ceram. Soc.*, 1994, **77**(10), 2632–2640.
24. Boutz, M. M. R., Winnubst, A. J. A. and Burggraaf, A. J., Yttria-ceria stabilized tetragonal zirconia polycrystals: sintering, grain growth and grain boundary segregation. *J. Eur. Ceram. Soc.*, 1994, **13**, 89–102.
25. Scott, M. G., Phase relationships in the zirconia–yttria. *J. Mater. Sci.*, 1975, **10**, 1527–1535.
26. Leung, D. K., Chan, C.-J., Ruhle, M. and Lange, F. F., Metastable crystallization, phase partitioning, and grain growth of ZrO_2–Gd_2O_3 materials processed from liquid precursors. *J. Am. Ceram. Soc.*, 1991, **74**(11), 2786–2792.
27. Lange, F. F., Transformation-toughened ZrO_2; correlations between grain size control and composition in the system ZrO_2–Y_2O_3. *J. Am. Ceram. Soc.*, 1986, **69**(3), 240–242.
28. Allemann, J. A., Michel, B., Märki, H.-B., Gaukler, L. J. and Moser, E. M., Grain growth of differently doped zirconia. *J. Eur. Ceram. Soc.*, 1995, **15**, 951–958.
29. Boutz, M. M. R., Nanostructured tetragonal zirconia ceramics. Microstructure, sinter forging and superplasticity. PhD thesis, University of Twente, Enschede, The Netherlands, 1993.
30. Upadhyaya, D. D., Bhat, R., Ramanathan, S., Roy, S. K., Schubert, H. and Petzow, G., Solute effect on grain growth in ceria ceramics. *J. Eur. Ceram. Soc.*, 1994, **14**, 337–341.
31. Longo, V. and Podda, L., Phase equilibrium diagram of the system ceria–yttria for temperatures between 900 and 1700°C. *J. Mater. Sci. Lett.*, 1981, **16**(3), 839–841.